Project Title:

***CATALYSIS SCIENCE INITIATIVE*:** From First Principles Design to Realization of Bimetallic Catalysts for Enhanced Selectivity

Grant Number: DE-FG02-03ER15469

Principal Investigator: Manos Mavrikakis (PI) – UW-Madison
Co-PI: James A. Dumesic - UW-Madison

1. Project Summary

In this project, we have integrated state-of-the-art Density Functional Theory (DFT) models of heterogeneous catalytic processes with high-throughput screening of bimetallic catalytic candidates for important industrial problems. We have studied a new class of alloys characterized by a surface composition different from the bulk composition, and investigated their stability and activity for the water-gas shift reaction and the oxygen reduction reaction. The former reaction is an essential part of hydrogen production; the latter is the rate-limiting step in low temperature H_2 fuel cells. We have identified alloys that have remarkable stability and activity, while having a much lower material cost for both of these reactions.

Using this knowledge of bimetallic interactions, we have also made progress in the industrially relevant areas of carbohydrate reforming and conversion of biomass to liquid alkanes. One aspect of this work is the conversion of glycerol (a byproduct of biodiesel production) to synthesis gas. We have developed a bifunctional supported Pt catalyst that can cleave the carbon-carbon bond while also performing the water-gas shift reaction, which allows us to better control the H_2:CO ratio. Knowledge gained from the theoretical metal-metal interactions was used to develop bimetallic catalysts that perform this reaction at low temperature, allowing for an efficient coupling of this endothermic reaction with other reactions, such as Fischer-Tropsch or methanol synthesis.

In our work on liquid alkane production from biomass, we have studied deactivation and selectivity in these areas as a function of metal-support interactions and reaction conditions, with an emphasis on the bifunctionality of the catalysts studied. We have identified a stable, active catalyst for this process, where the selectivity and yield can be controlled by the reaction conditions.

While complete rational design of catalysts is still elusive, this work demonstrates the power of combining the insights gained from theoretical models and the work of experiments to develop new catalysts for current and future industrial challenges.

2. Project Description:

I. Overview

"Catalysis by design" has been a dream for decades. To specify the composition and structure of matter to effect a desired catalytic transformation with predicted rate and selectivity remains a significant challenge, especially in heterogeneous catalysis. The goal of this project is to demonstrate a new paradigm for catalyst design. Our emphasis is on catalyst design for *selectivity*, with bimetallic systems providing the focus for our fundamental studies, synthetic strategies and design efforts.

The approach we have articulated is to enhance selectivity by design via the integration of four critical components: Theory and Modeling; Surface Science; Materials Synthesis, Characterization and Scale-up; and Catalyst optimization. Our studies in these areas have resulted in new catalysts for use in the areas described in our original proposal, including selective hydrogenation, selective oxidation, and selective carbohydrate reforming. In addition, using the principles garnered from our work in these areas, we have identified new catalysts in areas outside the scope of the original proposal. One example of this is our identification of new Near Surface Alloys (NSAs) for hydrogen transfer and water-gas shift reactions.

At the risk of obscuring such successes, we review our advancement of each of the critical catalyst design components.

II. Theory and modeling (Mavrikakis)

Synopsis: Modern computational chemistry tools such as Density Functional Theory (DFT) have emerged as powerful techniques for analysis and design in surface chemistry and catalysis. The focus of our efforts has been on the elucidation of trends in the chemical and catalytic properties of bimetallic surfaces for reaction of increasing complexity, and the identification of promising materials for specific selective reactions. The most extensive results of *ab initio* calculations are the development of the formalism of Near Surface Alloys (NSAs) and the determination of thermodynamic and kinetic parameters for simple reactions related to water gas shift (WGS) and other reactions (such as oxygen reduction) on these. Theory and modeling have a crucial role to play in the understanding of catalytic processes and the design of new catalysts; the challenge is to determine the necessary level of detail (and to have the appropriate tools at the desired level) to make the most effective use of these.

Near Surface Alloys and Hydrogen Binding

We have developed a first-principles-based approach for the identification of Near Surface Alloy (NSA) bimetallic catalysts stable in the presence of hydrogen. In particular, some of these surfaces bind hydrogen as weakly as the noble metals (Cu, Au), and yet activate H_2 far more easily than the noble metals. The unique combination of weak binding of the dissociation products with the low bond-breaking activation energy barrier opens new

possibilities for the design of highly selective *low temperature* hydrogen transfer catalysts. The NSA catalyst screening and identification approach developed is quite general, and we have started working towards identifying bimetallic catalysts that would be promising for a number of catalytic reactions, including water gas shift (WGS). The latter reaction is of central importance for the efficient Aqueous Phase Carbohydrate reforming towards H_2 and alkanes, recently developed at Wisconsin. In parallel, and in collaboration with BNL researchers, we have developed similar first-principles screening methods for identifying key reactivity descriptors for the Oxygen Reduction Reaction (ORR). Stable bimetallic and trimetallic NSAs designed on the basis of this work have yielded a current density increase of ca. 400%, compared to state-of-the-art all-Pt ORR electrocatalysts. These theoretical efforts also complement our ongoing surface science studies on surface reactions of bimetallics and provide useful guidance for our efforts to synthesize catalytic nanoparticles with precise atomic-scale architecture.

In the course of our systematic investigations of reaction selectivity as a function of the electronic structure of bimetallic surfaces, we developed a general framework for the identification of bimetallic NSAs which are stable in the presence of certain adsorbates and have unique properties in terms of their ability to catalyze specific reactions with high selectivity. In particular, using state-of-the-art DFT methods, we have recently identified a new class of alloys that exhibit superior catalytic behavior for hydrogen-transfer reactions. This class of materials, which we call Near-Surface Alloys (NSAs), is comprised of alloys wherein a solute metal is present near the surface of a host metal in concentrations different from the bulk. NSAs offer significant promise for nanoscale catalyst design. Indeed, single crystal investigations have already demonstrated some of the remarkable properties of these materials. For example, thin layers of platinum on Ru(0001) crystals dramatically reduce the strength of CO binding compared to pure Pt(111) surfaces. Similarly, a small amount of Ni deposited on both single crystal and catalytic Pt particles significantly decreases the desorption temperature of hydrogen compared to the respective pure metal surfaces. More specifically, using planewave DFT calculations and by adopting simple but realistic nanoscale models of *subsurface alloys* and *overlayer* structures, as shown in the insets of Figure 1, we first evaluated the stability of a large class of NSAs in H-rich environments.

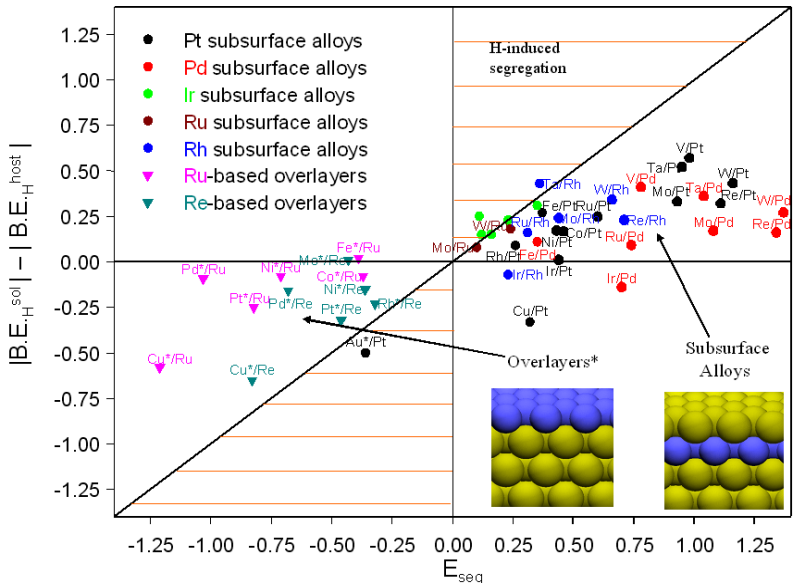

Figure 1: *Identifying NSAs stable in H-rich environments*

These initial calculations allow us to make a direct comparison *between* the segregation energy of the solute metal in the respective host metal *and* the difference in binding energy of H ($B.E._H$) between the two metals. If the $B.E._H$ to the element lying in the subsurface is much greater than that to the surface element, then that driving force might be sufficient to pull the subsurface element to the surface, and thus cause adsorbate-induced surface segregation. As a result, NSAs lying outside the hatched regions of Figure 1 are expected to retain their near surface structure in H-rich environments, and we focussed our subsequent analysis on this subset of NSAs.

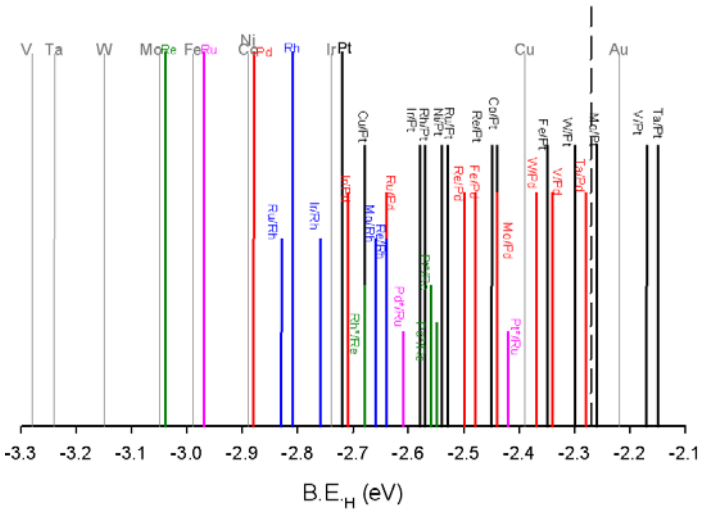

Figure 2: *Spectrum of H binding energies on various NSAs*

Figures 2 and 3 summarize the novel properties of H on the NSAs which were found to be stable in H-rich environments. Figure 2 gives the $B.E._H$ on NSA close-packed surfaces. We predict that NSAs provide opportunities for fine-tuning the $B.E._H$, and in particular, to bridge the gap in $B.E._H$ between the late transition metals and the coinage metals. Furthermore, we have identified NSAs that bind H more weakly than do Cu and Au. On conventional catalytic materials, weak binding of a dissociation reaction product would normally imply a higher dissociation barrier. However, as shown in Figure 3, NSAs offer the exciting opportunity to escape from that behavior, which limits conventional catalysts. Specifically, although some of these NSAs bind H as weakly as Cu and Au, they break the H-H bond far more easily (0.5-1.0eV lower transition state energy) than Cu and Au. This novel property suggests that specific NSAs should be able to activate H_2 easily, and at the same time bind H weakly, which translates to exciting possibilities for *low-temperature, highly selective*, hydrogen-transfer reactions.

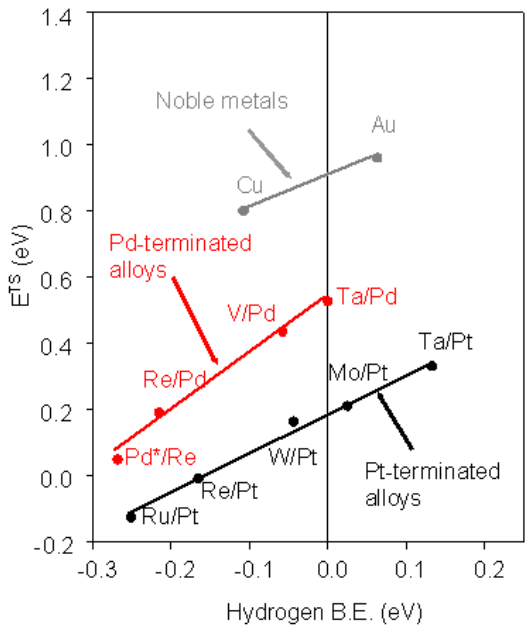

Figure 3 : *NSA's activate H_2 much easier than noble metals, and yet, bind H as weakly as the noble metals*

To take full advantage of these promising properties of NSAs, it is important to reproducibly prepare such NSA catalytic particles. Novel synthesis methods with atomic-scale control, discussed among our other research thrusts below, may provide a viable means of preparing layered NSA particles with unprecedented layer-by-layer

precision.

NSAs for Fuel-Cell Applications

An exciting application for NSAs not anticipated in our original proposal is in fuel cells. The Oxygen Reduction Reaction (ORR) has been shown in the literature to be the rate-limiting step for the entire reaction cycle of low temperature fuel cells. Current state-of-the-art ORR catalysts are made of pure Pt and, because of the price of Pt, they contribute to making fuel cells expensive. Our goal in this area has been (1) to decrease the amount of Pt in the cathode, (2) without compromising catalyst stability in a highly corrosive environment, and, (3) to possibly increase ORR rates, which translates into higher current densities produced by the fuel cell.

In collaboration with Dr. R. Adzic at BNL, we have launched a combined experimental/theoretical line of research, which has identified two key reactivity descriptors of the ORR, despite the fact that the exact reaction mechanism remains elusive. In the first paper, we decreased the amount of Pt substantially, by preserving only a monolayer (ML) of Pt supported on a variety of late transition metals (Ru, Ir, Rh, Au, Pd) (see fig 4). We found that a single ML of Pt supported on Pd(111) gave a catalyst that is 33% more active that the all-Pt(111) catalyst. The fundamental reason behind this rate enhancement was identified as the combined effect of strain and the electronic coupling between Pt and its respective substrate metal. Pd strikes an optimal balance for the activation energy barrier of the O-O bond-breaking and the O-H bond-making steps, both playing a key role in the overall ORR.

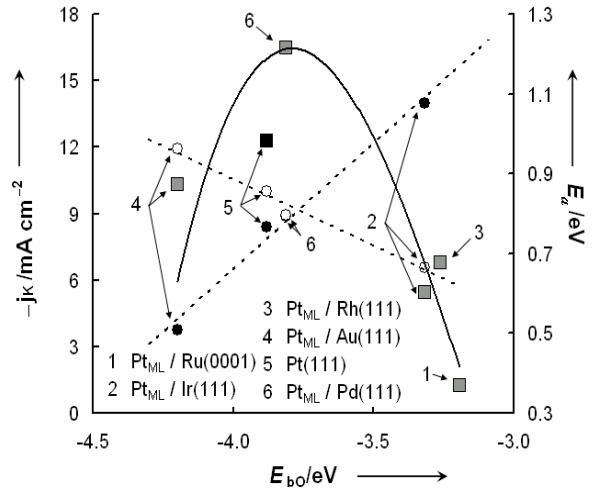

Figure 4 : *Maximizing ORR activity of Pt monolayers supported on other metals*

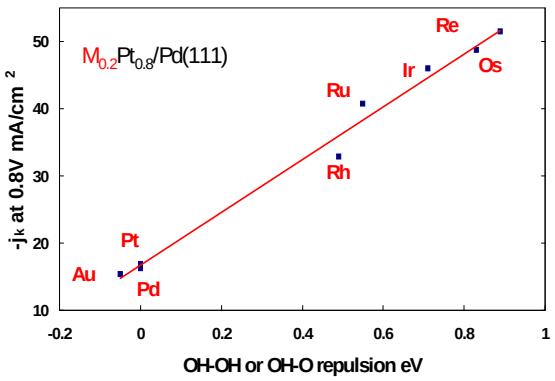

Figure 5 : *Pd-supported Pt_3M-monolayers can enhance ORR rates by up to 400%*

In a subsequent step, we kept Pd as the substrate of Pt, and we investigated the effect of replacing fraction of the Pt surface ML with a more reactive transition metal M (e.g.: Au, Pd, Rh, Ru, Os, Re). We found that the optimal composition for the surface ML was Pt_3M,

for all M studied, and that the current densities measured from these catalysts scale linearly with a new key reactivity descriptor we identified for ORR, namely the repulsion between the O or OH on M with the OH on an adjacent Pt site (see fig 5). For the case of Pt_3Re-ML on Pd(111), we not only decreased the Pt-mass used by about 20 times, but at the same time we obtained a ca. 400% increase in the resulting current density (compared to the all-Pt(111) case).

These results demonstrate the potential of first-principles methods for identifying key reactivity descriptors of complicated reactions and for guiding the synthesis of NSAs, with two or more metal components, with electronic properties tailored into maximizing specific reaction rates.

III. New Processes and Catalyst Development and Optimization (Dumesic)

Synopsis: In addition to the bimetallic catalyst synthesis and performance studies above, driven by first principles theory and experiments, we have pursued catalyst development efforts aimed at high impact processes; specifically, the development of new catalysts for carbohydrate reforming and liquid alkane production from biomass. This work has been enabled by high-throughput techniques developed in the Dumesic lab. Carbohydrate reforming has the potential to impact the production of hydrogen and other fuels from biomass. This study also demonstrates the potential of high-throughput experimentation in combination with techniques and fundamental information developed throughout our program, to impact areas of national need.

Advances in carbohydrate reforming catalysts

We have shown that glycerol can be converted to gas mixtures of H_2 and CO, which can be used to produce fuels and chemicals by Fischer-Tropsch and methanol syntheses, over platinum-based catalysts at temperatures from 498 to 620 K. These temperatures are lower compared to conventional gasification of biomass (e.g., 800 – 1000 K), allowing this endothermic conversion of glycerol to H_2:CO gas mixtures to be coupled with exothermic Fischer-Tropsch and methanol synthesis processes, providing low-temperature and energy-efficient routes for production of fuels and chemicals. This new low-temperature catalytic approach can be used to produce fuels and chemicals from waste glycerol streams that are currently generated as a by-product from the production of biodiesel, and this heat-integrated catalytic process can be used as a less energy-intensive alternative to processes that are currently used to convert starch-based materials to fuel-grade ethanol.

The low temperatures of our catalytic conversion of glycerol overlap the temperatures employed for Fischer-Tropsch and methanol syntheses, allowing the coupling between these processes. In particular, the conversion of glycerol to produce CO and H_2 takes place by the following stoichiometric reaction:

$$C_3O_3H_8 \longrightarrow 3CO+4H_2 \qquad (1)$$

The endothermic heat of this reaction corresponds to about 24% of the heating value of the glycerol. The exothermic heat generated by converting the CO and H_2 to liquid alkanes (*e.g.*, octane) by Fischer-Tropsch synthesis corresponds to about 28% of the heating value of the glycerol. Thus, coupling of glycerol conversion to synthesis gas with Fischer-Tropsch synthesis leads to the following exothermic process, with a heat that is about 4% of the heating value of the glycerol:

$$C_3O_3H_8 \longrightarrow \frac{7}{25}C_8H_{18} + \frac{19}{25}CO_2 + \frac{37}{25}H_2O \qquad (2)$$

One source of glycerol for our catalytic process is the low-value waste stream from transesterification of plant oils and animal fat to produce biodiesel, which contains glycerol in water at concentrations higher than 80%. Using this glycerol to produce methanol is an attractive alternative to help alleviate the burden of low-value waste glycerol and reduce production costs of biodiesel. Glycerol can also be produced by fermentation of sugars such as glucose, either as an alternative or as a by-product of the lingocellulose-to-ethanol industry. Unlike the fermentation of glucose to ethanol, which produces the final product at concentrations near 5 wt% in water, fermentation of glucose can be carried out to produce glycerol at concentrations of at least 25 wt%. This higher concentration of glycerol decreases the energy costs required to remove water from the oxygenated hydrocarbon fuel. Indeed, one of the most energy-intensive steps involved in the production of fuel-grade ethanol from glucose is the distillation step. For example, the energy required to vaporize a 5 wt% aqueous solution of ethanol (to estimate the energy of distillation) corresponds to 1.4 times the lower heating value of the ethanol product. In contrast, the energy required to vaporize a 25 wt% aqueous solution of glycerol corresponds to 0.33 times the lower heating value of the liquid alkane products (utilizing the exothermic heat of reaction 2).

Figure 6 shows results for gas-phase conversion of glycerol to synthesis gas over supported Pt catalysts at 623 K and atmospheric pressure of a feed solution containing 30 wt% glycerol in water. Catalysts consisting of Pt supported on Al_2O_3, ZrO_2, CeO_2/ZrO_2, and MgO/ZrO_2 exhibited deactivation during time-on-stream, whereas the Pt/C catalyst showed stable conversion of glycerol to synthesis gas for at least 30 h (Figure 6A). The catalyst with the most acidic support, Pt/Al_2O_3, showed a period of apparently stable catalytic activity, followed by a period of rapid catalyst deactivation. Because the reactor initially operates at 100% conversion, glycerol is present only in the upstream portion of the catalyst bed in the tubular reactor, and a deactivation-front moves from the reactor inlet to the outlet as olefinic species are formed from glycerol on acid sites associated with alumina, followed by deposition of coke from these species on Pt surface sites. The most basic catalyst support, MgO/ZrO_2, showed rapid deactivation for all times-on-stream. The most stable oxide-supported catalyst appears to be Pt on CeO_2/ZrO_2; however, the performance of this catalyst is inferior to that of Pt supported on carbon.

The different deactivation profiles displayed in Figure 6 for the various catalysts suggest that the support plays an important role in the deactivation process. Figure 6D shows the rate of formation of C_2-hydrocarbons (ethane and ethylene) normalized by the rate of H_2 production for the various supported Pt catalysts. Negligible amounts of C_2-hydrocarbons were formed on the Pt/C catalyst. In contrast, catalysts consisting of Pt supported on the various oxide supports formed measurable amounts of C_2-hydrocarbons, and the (C_2-TOF):(H_2-TOF) ratio

increases with time-on-stream. This behavior suggests that one of the modes of catalyst deactivation is caused by dehydration processes occurring on the oxide catalyst supports, leading to the formation of unsaturated hydrocarbon species that form carbonaceous deposits on the Pt surface, thereby decreasing the rate of H_2 production and thus increasing the (C_2-TOF):(H_2-TOF) ratio.

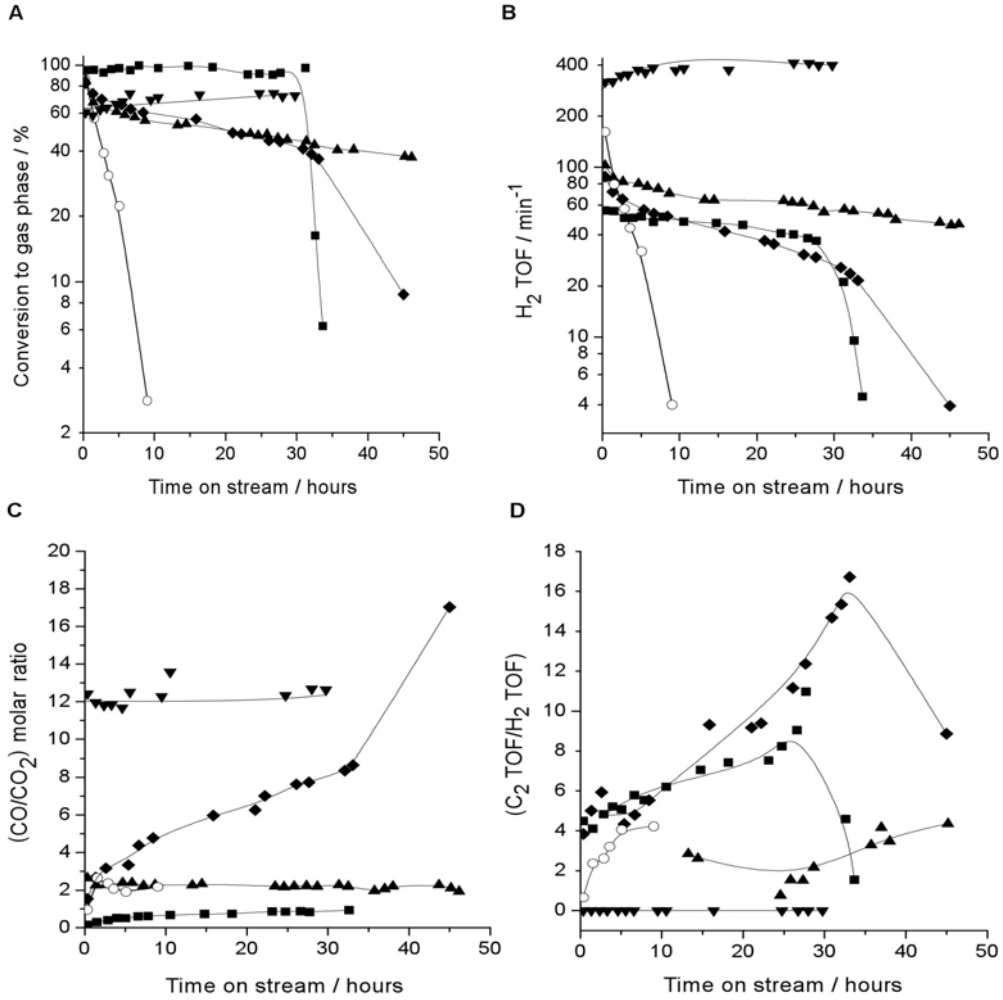

Figure 6: *Performance of supported Pt catalysts. Variation of* ***A)*** *conversion to gas phase products,* ***B)*** *H_2 turnover frequency,* ***C)*** *CO/CO_2 molar ratio, and* ***D)*** *C_2 to H_2 ratio for Pt catalysts supported on Al_2O_3 (■), CeO_2/ZrO_2 (▲), C (▼), ZrO_2 (♦), and MgO/ZrO_2 (○). Conversion to gas phase is calculated as (C atoms in gas phase product stream/total C into reactor as feed) x 100. Reactions carried out at 1 bar and 623 K with 0.32 cm^3 min^{-1} of 30 wt% aqueous-glycerol feed solution over 1.0 g of oxide-supported Pt catalysts or 0.060 g of Pt/C catalyst.*

The H_2:CO ratio for the product stream from the Pt/C catalyst is equal to approximately 1.3 (see Table 1), in agreement with the stoichiometry of reaction (1). In contrast, the H_2:CO ratios obtained over the other catalysts were higher than 1.5, indicating contributions from water-gas shift, WGS. This behavior is demonstrated more clearly by the CO:CO_2 ratio, as shown in Figure 6C. The initial CO:CO_2 ratio for Pt/C is 12, while it is less than 3 for the other catalyst. Thus, it appears that the WGS reaction is facilitated by the presence of the oxide support.

Reaction conditions (see Table 1) leading to lower conversions of glycerol (*i.e.*, higher flow rates of the 30 wt% glycerol feed and higher glycerol concentrations at constant feed flow rate) lead to higher $CO:CO_2$ ratios. This behavior suggests that the primary reaction in glycerol conversion is the formation of CO and H_2, and the production of CO_2 by WGS is a secondary reaction. The important consequence of this behavior is that it is possible to adjust the space velocity of the catalytic process to ensure that the conversion of glycerol is complete and yet to control the H_2:CO ratio for the Fischer-Tropsch synthesis step.

The results in Table 1 show that the rate of H_2 production passes through a maximum with respect to reaction temperature at constant feed conditions. The rate increases with increasing temperature from 573 to 623 K (with an activation energy barrier of about 70 kJ/mol). In contrast, while the rate of hydrogen production increases further when the temperature is initially increased to 673 K, the Pt/C catalyst begins to undergo deactivation versus time-on-stream at this higher temperature. We suggest that dehydration processes are too fast compared to H_2 formation reactions at higher temperatures, leading to catalyst deactivation.

Table 1: *Experimental data for catalytic conversion of glycerol at various conditions*

Process Conditions		Conversion to gas phase (%)	H_2 TOF (min^{-1})	H_2/CO	CO/CO_2	CH_4/H_2
Feed flow rate (cm^3 min^{-1})[a]	0.08	68	111	1.6	5.7	0.038
	0.16	71	241	1.4	8.8	0.036
	0.32	64	373	1.3	12	0.045
	0.64	39	449	1.3	17	0.038
Glycerol concentration (wt%)[b]	20	64	265	1.4	8.7	0.025
	30[c]	50	285	1.3	14	0.032
	50	26	267	1.2	37	0.050
Temperature (K)[d]	573	17	104	1.31	90	0.037
	623	54	335	1.31	17	0.027
	673	100	600	1.33	11	0.027
	673[e]	72	450	1.38	-	-
	723	61	419	1.68	4.6	0.019
	723[e]	43	300	1.83	-	-

For these reaction kinetics studies, 0.060 g of 5 wt % Pt/C was used. [a] Glycerol feed concentration of 30 wt %, 623 K, and 1 bar. [b] Feed flowrate of 0.32 cm^3 min^{-1}, 623 K, and 1 bar. [c] Point taken after 2 h time-on-stream. [d] Glycerol feed concentration of 30 wt % at 0.32 cm^3 min^{-1} and 1 bar. [e] Point taken after 3 h time-on-stream.

Figures 7A and 7B show the performance of the Pt/C catalyst at increased pressure (from 1 to 20 bar) for the 30 wt% glycerol feed, and for increased glycerol feed concentration (from 30 to 50 wt%) at a pressure of 1 bar. The catalyst showed good stability for at least 48 h time-on-stream for both the higher glycerol feed concentration (50 wt%) and the higher

reaction pressure (20 bar). The Pt/C catalyst shows excellent stability for converting a 30 wt% glycerol feed to produce synthesis gas at 20 bar with a H_2:CO ratio (equal to approximately 2) that is appropriate for Fischer-Tropsch or methanol synthesis.

To achieve efficient coupling of the endothermic conversion of glycerol to synthesis gas with the exothermic Fischer-Tropsch or methanol synthesis steps, it is beneficial to achieve glycerol conversion at the lowest possible temperature. In addition, conducting glycerol conversion at lower temperatures allows for flexibility in the choice of the Fischer-Tropsch technology used to convert the synthesis gas to liquid alkanes (e.g., Co-based versus Fe-based catalysts). Therefore, we carried out studies of glycerol conversion to synthesis gas at temperatures from 498 to 573 K. The catalytic conversion of polyols to H_2, CO_2 and CO

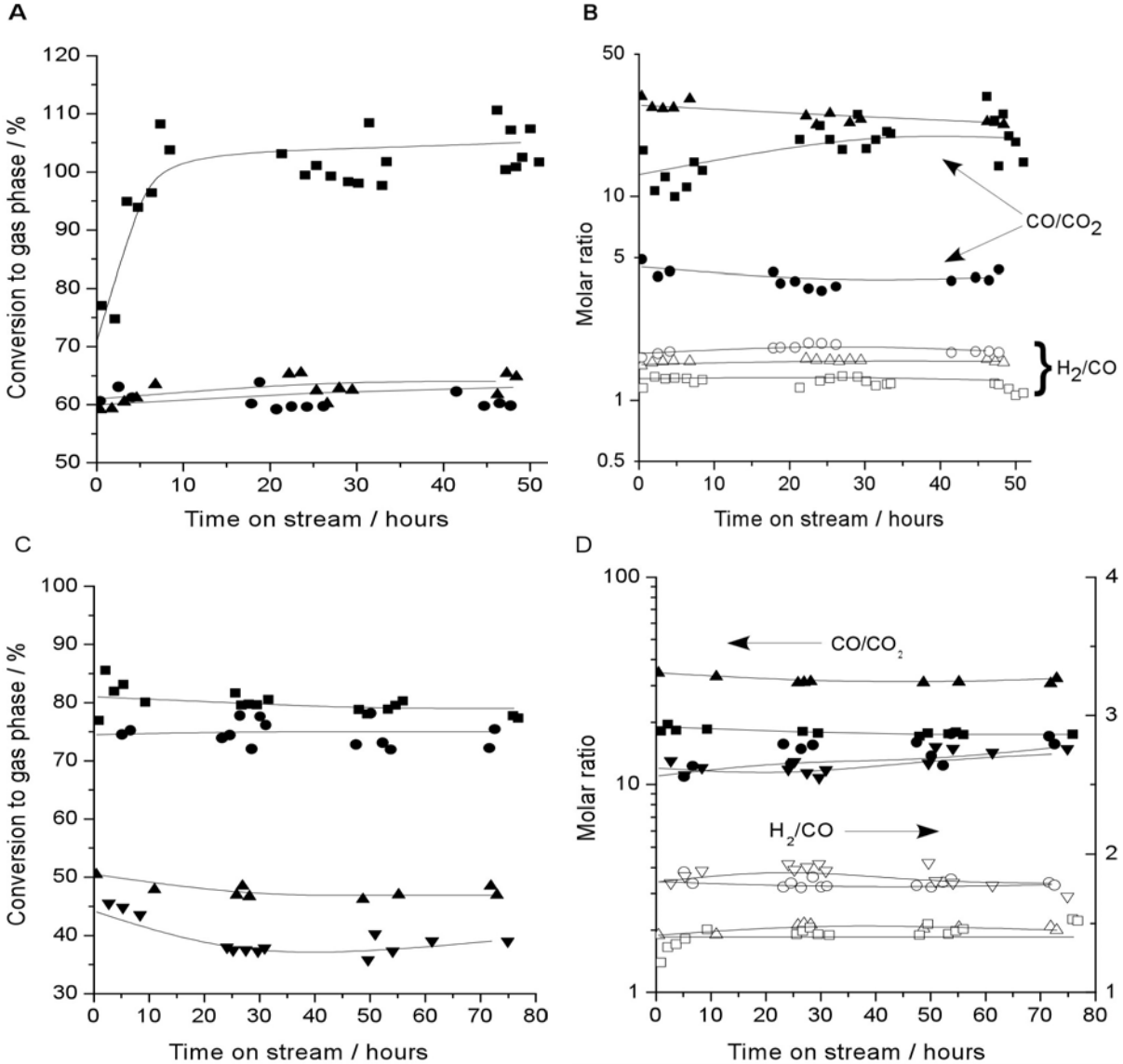

Figure 7: *Performance of carbon supported Pt and Pt-bimetallic catalysts at various process conditions. Variation of* ***A)*** *glycerol conversion to gas phase products and* ***B)*** *molar ratios for conversion of 30 wt% glycerol at 1 bar (■), 50 wt% glycerol at 1 bar (▲), and 30 wt% glycerol at 20 bar (●) over 0.090 g Pt/C at 623 K. Variation of* ***C)*** *glycerol conversion to gas phase products and* ***D)*** *CO/CO_2 (closed symbols) and H_2/CO (open symbols) molar ratios for conversion of 30 wt%*

*glycerol at 1 bar over Pt:Ru/C at 548 K (triangles; 0.435 g catalyst) and 573 K (squares; 0.513 g catalyst) and over Pt:Re/C at 498 K (inverse triangles; 0.535 g catalyst) and 523 K (circles; 0.535 g catalyst). A feed rate of 0.16 cm^3 min^{-1} for **A** and **B** and 0.08 cm^3 min^{-1} for **C** and **D** was used*

involves the preferential cleavage of C-C bonds compared to C-O bonds, and Pt-based catalysts are particularly active and selective for this process. Under these reaction conditions, we have shown earlier that the surface is covered primarily by adsorbed CO species; therefore, a strategy to produce a catalyst that is active at low temperatures for the conversion of polyols to synthesis gas is to facilitate the desorption of CO into the gas phase, thereby suppressing the subsequent water-gas shift step and turning over the catalytic cycle by regenerating vacant surface sites. Accordingly, we require materials that possess the catalytic properties of Pt with respect to selective cleavage of C-C versus C-O bonds, but that have weaker heats of CO adsorption, as can be achieved using Pt-Ru and Pt-Re alloy catalysts.

Figures 7C and 7D show that the conversion of glycerol and the product gas ratios remain constant for at least 72 h time-on-stream at these low temperatures over Pt:Ru and Pt:Re bimetallic catalysts (with atomic ratios of 1:1). The main condensable organic species in the effluent streams of the catalysts were unconverted glycerol, with smaller amounts of ethylene glycol, methanol, acetic acid, and ethanol. These results demonstrate that the conversion of glycerol to synthesis gas can, in fact, be accomplished at temperatures well within the temperature ranges employed for Fischer-Tropsch and methanol syntheses, allowing for efficient coupling between these processes. Moreover, we have shown that the H_2/CO ratio can be adjusted by adding a WGS functionality.

Production of Liquid Alkanes from Biomass

Another process which may find benefit from bimetallic catalysts is the production of liquid alkanes from biomass. We have explored bi-functional catalysts containing basic and mono-metallic sites that carry out aldol-condensation and hydrogenation. These are candidates for bimetallics during the next phase of this research. The motivation for this work arises from the interest in replacement of petroleum fuels in the transportation sector with liquid, biomass- derived fuels that can use the existing delivery infrastructure, while not needing extensive vehicle engine modification. Recently, we developed a process that produces liquid alkanes by aqueous-phase processing of biomass-derived carbohydrates. Alkane products from this process have high cetane numbers, making them excellent blending agents to produce sulfur-free diesel fuel for transportation applications.

Our process to convert renewable biomass-derived carbohydrates to alkanes with molecular weights in the range of diesel fuel (C_7 to C_{15}) starts with acid-catalyzed dehydration of carbohydrates to form carbonyl groups, followed by aldol-condensation over a solid base catalyst (such as mixed Mg-Al-oxide) to form C-C bonds, and subsequent hydrogenation of C=C and C=O bonds over a metal catalyst (such as Pd/Al_2O_3) to form large water-soluble organic compounds. These molecules are then converted to liquid alkanes by aqueous-phase dehydration/hydrogenation (APD/H) reactions over a bifunctional catalyst containing acid and metal sites in a flow-reactor with two feed streams: an aqueous stream containing the organic reactant and a hexadecane sweep stream. During the past year, we have

demonstrated that aldol-condensation and hydrogenation steps can be combined in a single-reactor using a bifunctional Pd/MgO-ZrO_2 catalyst that has high activity and selectivity, as well as excellent recyclability and hydrothermal stability.

Figure 8 shows the bifunctional reaction pathways involved in the production of large, water-soluble molecules from biomass-derived furfural or 5-hydroxymethylfurfural, HMF (from xylose or glucose, respectively). In this example, the base catalyst abstracts an α-H atom from acetone to form a carbanion intermediate which then attacks the carbon atom of the carbonyl group of furfural to form a C-C bond. Molecules such as furfural or HMF cannot form carbanion intermediates for aldol-condensation because they do not have α-H atoms. This reaction between furfural and acetone results in formation of a C_8 species that undergoes dehydration to form an α-β unsaturated aldehyde (monomer) species, which has limited solubility in water. The C_8 monomer can further condense with a second furfural molecule to form a dehydrated C_{13} aldol-adduct (dimer), which has even lower solubility in water. Following these aldol-condensation reactions, hydrogen is introduced into the reactor, leading to hydrogenation of the furan rings in the aldol-adducts over the metallic sites on the catalyst, thereby increasing the solubility of the products in water to levels higher than 35 wt%. An analogous series of reactions can be depicted for HMF, leading to the formation of C_9 and C_{15} molecules.

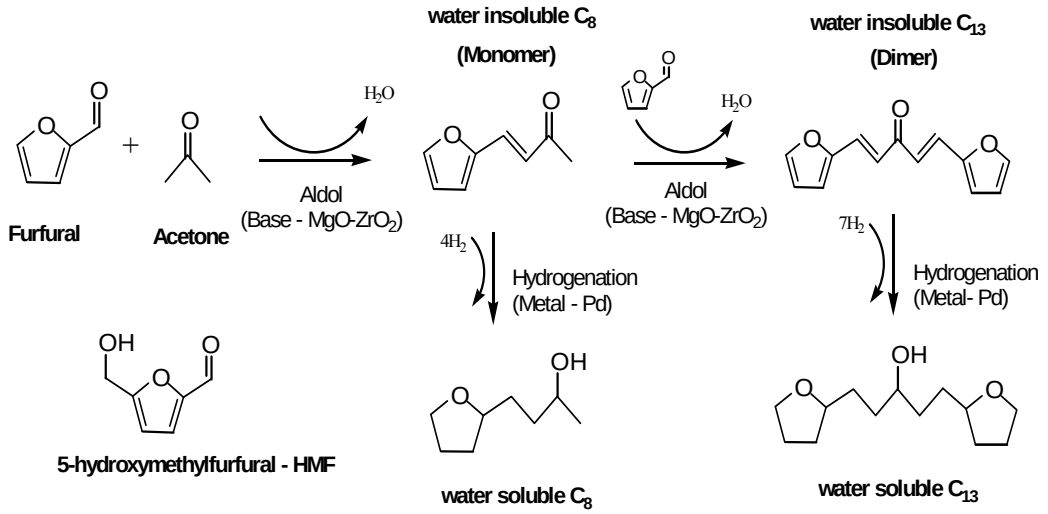

Figure 8: *Reaction network for aldol-condensation of furfural (or HMF) and acetone, followed by hydrogenation of aldol-adducts*

In previous work, we carried out aldol-condensation reactions using a mixed Mg-Al-oxide catalyst derived from hydrotalcite synthesis, and we added a Pd/Al_2O_3 catalyst to carry out the subsequent hydrogenation step in a batch reactor. However, the mixed Mg-Al-oxide catalyst lost approximately 79% and subsequently 96% of its initial activity after the second and third uses of this catalyst for the aldol-condensation of HMF with acetone (HMF:acetone ratio of 1:10). This loss of activity persisted after calcination of the catalyst between recycle runs. In addition, the mixed Mg-Al-oxide catalyst when physically mixed with Pd/Al_2O_3 showed a 15% loss of selectivity to formation of dimer and a 10% loss in overall carbon yield, thereby indicating a negative effect of the Pd/Al_2O_3 catalyst on the performance of the mixed Mg-Al-oxide catalyst for aldol-condensation. In contrast, the

$MgO\text{-}ZrO_2$ catalyst exhibited excellent recyclability upon repeated use for aldol-condensation reactions in the aqueous phase.

Figure 9 shows the aqueous phase concentration of carbon (normalized to the initial concentration of carbon in the batch reactor) versus time during aldol-condensation over a bifunctional $Pd/MgO\text{-}ZrO_2$ catalyst at various temperatures, followed by sequential hydrogenation in the same batch reactor at 393 K. As aldol-condensation proceeds, monomer and dimer species form and precipitate out of the solution, and the amount of carbon in the aqueous phase decreases accordingly. During this reaction the Pd on the catalyst is inert, because the performance of the $Pd/MgO\text{-}ZrO_2$ catalyst is identical to the performance of $MgO\text{-}ZrO_2$ during aldol-condensation. On average 80% of the furfural has disappeared after a period of 24 h under these reaction conditions. The reactor is then pressurized to about 55 bar with hydrogen to initiate subsequent hydrogenation of the furan rings and thereby increase the solubility of monomer and dimer species in the aqueous phase. As seen in Figure 10, this hydrogenation step leads to an increase in the concentration of carbon in the liquid phase. For example, while the carbon concentration in the aqueous phase after aldol-condensation at 326 K decreases to about 44% of the initial carbon concentration, this value increases to about 94% after the hydrogenation step. This figure illustrates the ability of the bifunctional $Pd/MgO\text{-}ZrO_2$ catalyst to facilitate a single-reactor, aqueous phase process that combines aldol-condensation with sequential hydrogenation, in which the aqueous phase carbon lost during the aldol-condensation step is returned to the aqueous phase during the hydrogenation step.

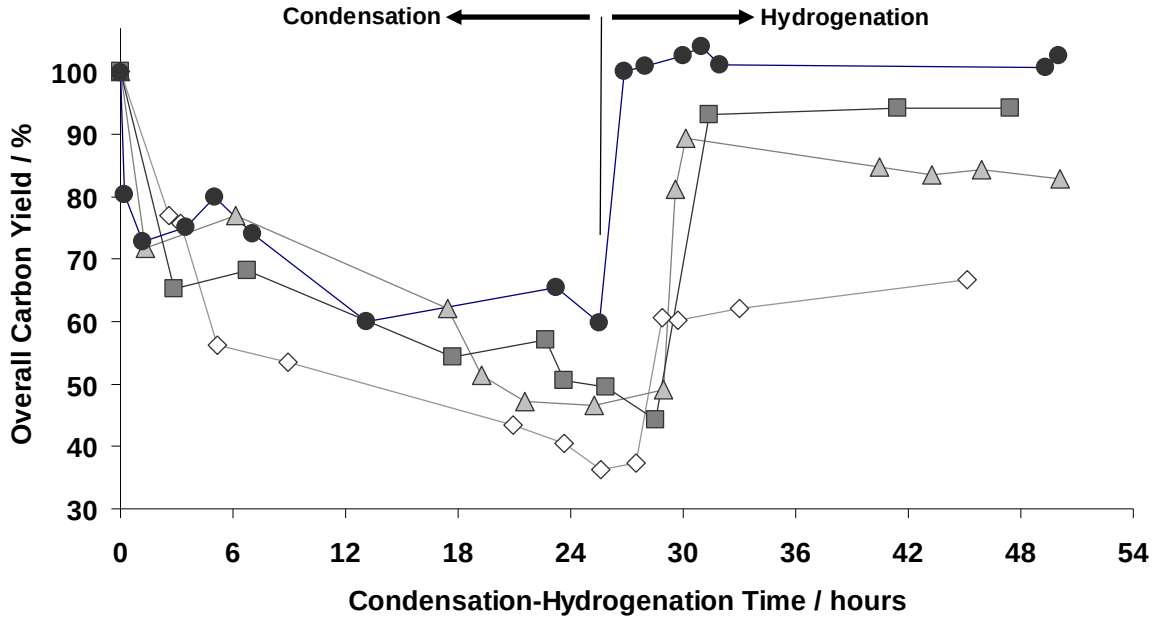

Figure 9: *Overall carbon yield in the aqueous phase versus time for aldol-condensation at various temperatures of HMF with acetone (HMF:acetone molar ratio equal to 1:1), followed by hydrogenation at 393 K. (Black Circles) 298 K, (Dark Grey Squares) 326 K, (Light Grey Triangles) 353 K, (White Diamonds) 393 K.*

Experiments were conducted to study the stability and recyclability of the bifunctional 5 wt% Pd/MgO-ZrO_2 for aldol-condensation of acetone with furfural (molar ratio of 1:1) at 326 K, followed by hydrogenation at 393 K. The catalyst was recycled for use in runs 2 and 3 without any intermediate regeneration, whereas the catalyst was subjected to a calcination treatment prior to run 4. Figure 10A shows that selectivity for the formation of the dimer adduct decreases by about 18% for recycle runs 2 and 3, while still maintaining good overall carbon yield (>90%). The CO and CO_2 chemisorption uptakes to titrate metallic and basic sites (49 and 103 μmol/g, respectively) and the BET surface area of the catalyst (280 m^2/g) did not change appreciably (by less than 10%) for the recycled catalyst. Hence, the catalyst shows excellent recycling ability and hydrothermal stability.

Figure 10B shows experimental results obtained at temperatures from 298 to 393 K for aldol-condensations of furfural with acetone at a molar ratio of 1:1. The rate of reaction increases with temperature; however, the overall carbon yield in the aqueous solution after aldol-condensation (followed by hydrogenation) decreases at temperatures above 353 K, probably due to the formation of coke on the catalyst during aldol-condensation. As the temperature is increased from 326 to 353 K, the selectivity for dimer increases by 17% with no significant change in the overall carbon yield. In contrast, as the temperature is increased further from 353 to 393 K, the dimer selectivity remains the same but the overall carbon yield decreases by 8%. Thus, it appears that the optimum temperature for aldol-condensation of furfural is near 353 K, with this temperature providing a compromise between the selectivity for heavier product and overall carbon yield. In the case of aldol-condensation between HMF and acetone (Figure 10C), the optimum temperature for aldol-condensation is near 326 K. At these optimum temperatures, the furfural:acetone reaction achieves a higher final conversion by 16%, but a lower dimer to monomer ratio (1.8 versus 3.4) as compared to the HMF:acetone reaction. Results in Figure 10D show that the molar ratio of reactants for aldol-condensation plays a significant role in controlling the reaction selectivity. The presence of excess acetone (furfural:acetone molar ratio of 1:9) leads primarily to the formation of monomer. When the molar ratio of furfural:acetone is increased from 1:9 to 1:1, the selectivity for the formation of dimer species increases by 31%, and this selectivity increases further by 12% when the furfural:acetone ratio increases from 1:1 to 2:1.

Aldol-condensation does not take place homogeneously in the aqueous phase by dissolved basic species, because the rate of aldol-condensation was negligible after the MgO-ZrO_2 catalyst was removed from the aqueous solution. Increasing the organic/catalyst mass ratio from 6 to 36 does not have an effect on the selectivity or the overall carbon yield of the process. Decreasing the amount of Pd on the MgO-ZrO_2 catalyst from 5 to 0.5 wt% increased by about an order of magnitude the time required to reach high overall yields of carbon in the aqueous phase at 393 K (i.e., from 5 to nearly 40 h). In another experiment, the aqueous solution was removed at the end of the aldol-condensation step, leaving the insoluble monomer and dimer species on the catalyst surface; and the reactor was then filled with hexadecane, followed by treatment in hydrogen at 393 K. This treatment led to the formation of hydrogenated monomer and dimer species in the hexadecane solvent, with an overall carbon yield of around 68%, indicating that the hydrogenated form of monomer and

dimer can be blended with diesel fuel without the need to convert these species into alkanes, thereby eliminating the need for the further APD/H processing step.

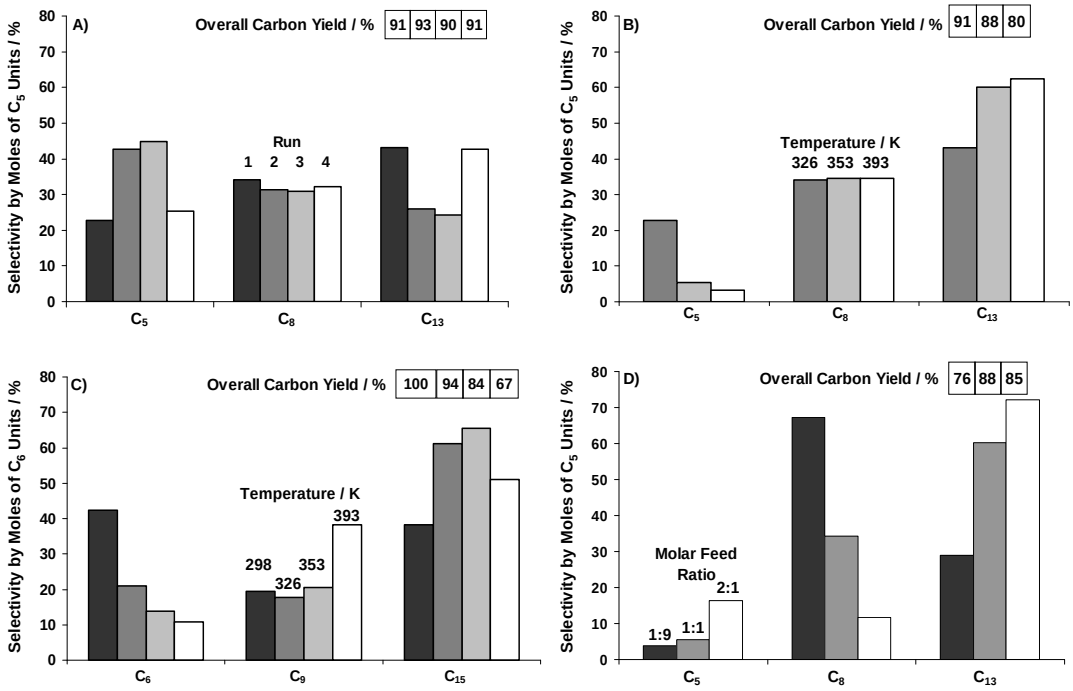

Figure 10: *Selectivity for C_5 (furfural:acetone) or C_6 (HMF:acetone) units in the aqueous phase after aldol-condensation followed by hydrogenation over 5 wt% Pd/MgO-ZrO_2 catalyst. C_5 selectivity = (moles C_5)*100/(moles C_5 + moles C_8 + 2*moles C_{13}), with analogous definition for C_6 basis.* ***A)*** *Furfural:acetone (molar ratio of 1:1) over fresh and recycled catalyst. 5 wt% organics in aqueous phase; 326 K and 10 bar He for condensation and 393 K and 55 bar H_2 for hydrogenation; organic/catalyst mass ratio of 6, except run 4 which had a ratio of 9. (Bar 1 black) fresh catalyst with calcination, (Bar 2 dark grey) first recycle without calcination, (Bar 3 light grey) second recycle without calcination, (Bar 4 white) third recycle with calcination.* ***B)*** *Furfural:acetone (molar ratio of 1:1) over fresh catalyst at various condensation temperatures followed by hydrogenation at 393 K.* ***C)*** *HMF:acetone (molar ratio of 1:1) over fresh catalyst at various condensation temperatures followed by hydrogenation at 393 K.* ***D)*** *Various furfural:acetone molar ratios over fresh catalyst at 353 K for condensation followed by hydrogenation at 393 K.*

Overall, we have shown that Pd/MgO-ZrO_2 is an active, selective, and hydrothermally stable catalyst for aldol-condensation over basic sites (MgO-ZrO_2) followed by sequential hydrogenation over metal sites (Pd). This bifunctional catalyst thus allows carbohydrate-derived compounds, like furfural and HMF, to be converted in a single reactor to large water-soluble intermediates for further aqueous phase processing to produce liquid alkanes. The selectivity and overall yield of the process can be controlled by the reaction temperature and the molar ratio of the aldol-condensation reactants. This aqueous phase process is still in its infancy, and it is likely that this process can be applied to other biomass-derived compounds containing carbonyl compounds, such as replacing acetone with glyceraldehyde or dihydroxyacetone.

IV. Summary

As demonstrated by the results above and the list of publications below, this program has been highly productive. We have made significant progress in both theoretical modeling and experimental catalyst development toward problems central to the DOE mission. By applying an understanding of the principles involved to the catalytic problems studied, we have designed and synthesized new catalysts that show promise for a variety of industrially relevant problems.

Graduate Student and Post-doctoral Researchers Supported

George Huber (PhD 2005)
Jeff Greeley (PhD 2004)
Ye Xu (PhD 2004)
Shampa Kandoi (PhD 2006)
Anand Nilekar
Chris Barrett

Publications Resulting from this Program

1. S. Kandoi, A. A. Gokhale, L. C. Grabow, J. A. Dumesicand M. Mavrikakis, "Why Au and Cu are more selective than Pt for preferential oxidation of CO at low temperature", Catalysis Letters 93, 93 (2004).

2. J. Greeley and M. Mavrikakis, "Competitive paths for methanol decomposition on Pt(111)", Journal of the American Chemical Society 126, 3910 (2004).

3. G. W. Huber, R. D. Cortright and J. A. Dumesic, "Renewable alkanes by aqueous-phase reforming of biomass-derived oxygenates", Angewandte Chemie International Edition 43, 1549 (2004).

4. J. Greeley, W. P. Krekelberg and M. Mavrikakis, "Strain-induced formation of subsurface species in transition metals", Angewandte Chemie International Edition 43, 4296 (2004).

5. J. Greeley and M. Mavrikakis, "Alloy catalysts designed from first principles", Nature Materials 3, 810 (2004).

6. A. A. Gokhale, G. W. Huber, J. A. Dumesic and M. Mavrikakis, "Effect of Sn on the reactivity of Cu surfaces", Journal of Physical Chemistry B 108, 14062 (2004).

7. A. A. Gokhale, S. Kandoi, J. P. Greeley, M. Mavrikakis and J. A. Dumesic, "Molecular-level descriptions of surface chemistry in kinetic models using density functional theory", Chemical Engineering Science 59, 4679 (2004).

8. R. R. Davda. J. W. Shabaker, G. W. Huber, R. D. Cortright and J. A. Dumesic, "A review of catalytic issues and process conditions for renewable hydrogen and alkanes by aqueous-phase reforming of oxygenated hydrocarbons over supported metal catalysts", Applied Catalysis B 56, 171 (2005).

9. N. Schumacher, A. Boisen, S. Dahl, A. A. Gokhale, S. Kandoi, L. C. Grabow, J. A. Dumesic, M. Mavrikakis and I. Chorkendorff, "Trends in low-temperature water-gas shift reactivity on transition metals", Journal of Catalysis 229, 265 (2005).

10. J. Greeley and M. Mavrikakis, "Surface and subsurface hydrogen: Adsorption properties on transition metals and near-surface alloys", Journal of Physical Chemistry B 109, 3460 (2005).

11. J. Zhang, M. B. Vukmirovic, Y. Xu, M. Mavrikakis and R. R. Adzic, "Controlling the catalytic activity of platinum-monolayer electrocatalysts for oxygen reduction with different substrates", Angewandte Chemie International Edition 44, 2132 (2005).

12. G. W. Huber, J. N. Chheda, C. J. Barrett and J. A. Dumesic, "Production of liquid alkanes by aqueous-phase processing of biomass-derived carbohydrates", Science 308, 1446 (2005)

13. J. Zhang, M.B. Vukmirovic, K. Sasaki, A.U. Nilekar, M. Mavrikakis and R.R. Adzic, "Mixed-metal Pt monolayer electrocatalysts for enhanced oxygen reduction kinetics", Journal of the American Chemical Society 127, 12480 (2005).

14. Y. Xu, J. Greeley and M. Mavrikakis, "Effect of subsurface oxygen on the reactivity of the Ag(111) surface", Journal of the American Chemical Society 127, 12823 (2005).

15. G. W. Huber and J. A. Dumesic, "An overview of aqueous-phase catalytic processes for production of hydrogen and alkanes in a biorefinery", Catalysis Today 111, 119 (2006).

16. R. R. Soares, D. A. Simonetti and J. A. Dumesic, "Glycerol as a source for fuels and chemicals by low-temperature catalytic processing", Angewandte Chemie International Edition, 45, 3982 (2006).

17. C. J. Barrett, J. N. Chheda, G. W. Huber and J. A. Dumesic, "Single-Reactor Process for Sequential Aldol-Condensation and Hydrogenation of Biomass-Derived Compounds in Water", Applied Catalysis B – Environmental 66, 111 (2006).

Recognition and Awards:

Jim Dumesic

- Cross-Canada Lectureship (2005)
- Plenary Lecturer, 6th Netherlands Catalysis and Chemistry Conference, Amsterdam (2005)
- Schuit Lecture, Technical University of Eindhoven (2005)
- Harry G. Fair Lecture, University of Oklahoma (April 2005)
- Keynote lecture at North American Catalysis Society meeting (2005)
- Distinguished Catalyst Researcher Seminar, Pacific Northwest National Laboratory (2005)
- Lind Lecturer, University of Tennessee/Oak Ridge National Laboratory (2005)

Manos Mavrikakis

- Samuel C. Johnson Distinguished Fellowship (2005-2008).
- Featured in: **Chemical & Engineering News**, Nov. 29, 2004, Vol. 82, Issue 48, pp. 25-28.
- Cited in: **Chemical & Engineering News**, Aug. 22, 2005, Vol. 83, Issue 84, pp. 42-47.
- Press Release by **NATURE MATERIALS:** October 17, 2004 – Designer Catalysts for Hydrogen Chemistry.
- Featured in Italian Newspaper: **IL-SOLE 24 ORE** (p. 11, 10/20/2004)
- Featured in **Reactive Reports**, March 2005 issue: **http://www.reactivereports.com/44/44_1.html**
- Featured in **EMSL – Pacific Northwest Laboratory Research Highlights** (January/February 2005): http://www.emsl.pnl.gov/new/highlights/200502/
- Featured in **Council on Competitiveness: High Performance Computing and Competitiveness-Grand Challenge Case Study:** *Customized Catalysts to Improve Crude Oil Yields: Getting More bang from Each Barrel* (April 2005): http://www.compete.org/pdf/HPC_Customized_Catalysts.pdf
- Featured in the *Nanotechnology* section of **MIT Technology Review** (June 2005): http://www.technologyreview.com/articles/05/06/issue/ftl_nano.asp?p=2
- Featured in **DOE-BES Computational Research 2005 Greenbook**: http://www.nersc.gov/news/greenbook/N5greenbook-print.pdf
- Keynote speaker, 18th Canadian Symposium on Catalysis, Montreal (2004)
- Keynote speaker, 23rd ECOSS conference, Berlin, Germany (2005).
- Keynote Lecture, 11th International Conference on Theoretical Aspects of Catalysis, Berlin, Germany, 2006.